Electron-hole-droplet dragging by phonon wind and exciton-condensation kinetics in germanium

N. V. Zamkovets, N. N. Sibel'din, S. G. Tikhodeev, and V. A. Tsvetkov

P. N. Lebedev Physics Institute, USSR Academy of Sciences

The kinetics of exciton condensation in the presence of a phonon wind produced by a stationary phonon source that is external to the cloud of electron-hole droplets (EHD) and excitons is investigated theoretically and experimentally. Equations are obtained for the exciton condensation and for the creation and growth of the moving drops. These equations are solved numerically. The volume of the liquid and gas phases, and the density and radii of EHD in germanium, are measured as functions of the phonon-wind intensity and of the crystal temperature.

INTRODUCTION

It was found in the last few years that a large number of properties of an electron-hole-droplet (EHD) system is determined by the interaction of the droplets with nonequilibrium phonons—with the phonon wind.[1,2] Intense fluxes of nonequilibrium phonons are produced both inside each EHD as a result of nonradiative recombination of the electron-hole pairs bound in the droplet, and in the region where the crystal is excited by thermalization of the nonequilibrium carriers produced by the pump source. The phonons are absorbed by the EHD (Refs. 1–4), to which they transfer their quasimomentum. The resultant drag force causes the EHD to drift at a velocity that increases with increasing excitation level and with decreasing temperature.[1,3,5–11] The droplet motion caused by the phonon wind is responsible for the spatial structure of the droplet cloud[11–14] and determines its dimensions,[1,7,12,14–18] its position in the crystal,[5,6,9,12,14,19] and its kinetics[1),4–6,8,9,12,17–21]

Under typical experimental conditions the excitation intensity is such that the EHD are moved by the phonon wind out of the generation region into an unexcited part of the crystal. Further growth of the produced critical nuclei occurs therefore in the course of their motion. After reaching the steady-state size, the droplet continues to move through the exciton cloud,[2)] which it subsequently leaves. At the same time, new EHD continue to be nucleated in the exciton cloud. Thus, under stationary excitation and at sufficient intensity of the phonon wind, different generations of EHD constantly replace one another.

Obviously, EHD motion must be taken into account in the description of exciton-condensation kinetics.[25] Condensation kinetics was considered in Refs. 26–32.[3)] These studies were performed, however, prior to the observation of droplet dragging by nonequilibrium phonons, and this effect was thus not taken into account there. The results of the cited papers can therefore be used to explain experiments performed at relatively low pump levels (e.g., experiments subject to hysteresis[32,33,35,36]), in which the effect of the phonon wind is insignificant.

In the present paper we use the approach developed in Ref. 28 to investigate exciton-condensation kinetics under phonon-wind conditions. Equations are obtained for the condensation in the case when the phonon wind is produced by a source external to the exciton cloud and to the EHD. The calculation is performed for two situations: condensation in a uniformly pumped semi-infinite crystal, and condensation with pumping in a limited region having smooth boundaries. We note that the equations obtained describe the condensation kinetics for any droplet drift-motion mechanism (motion in an inhomogeneous strain field,[37,38,22] dragging by ultrasound,[39,22] and others).

The condensation kinetics for phonon generation by an external source was investigated by light-scattering and luminescence methods. We measured the dependences of the sizes and densities of the EHD in liquid- and gas-phase volumes on the phonon-wind intensity and on the crystal temperature. The results confirm the main conclusions of the theory.

THEORY

We consider a one-dimensional situation: we assume that the phonon flux is spatially uniform and directed along the positive x axis, while the rate $g(x)$ of bulk generation of phonons is independent of the coordinates y and z. We confine ourselves to the steady state, i.e., we assume that all the quantities that enter in the problem are independent of time.

We write first an equation for the exciton-gas density $n(x)$, which we shall assume to be a sufficiently smooth function.[4)] In particular, we disregard the fact that the exciton density near each EHD is somewhat lower, i.e., we neglect exciton diffusion towards the EHD surface.[28] This equation takes the form[40,28,34]

$$-\frac{n(x)}{\tau} + g(x) + D\frac{d^2n(x)}{dx^2} - S_\Sigma(x) = 0, \qquad (1)$$

where τ and D are respectively the lifetime and the diffusion coefficient of the excitons, $S_\Sigma(x)$ is the rate of exciton condensation into a liquid phase per unit volume of the exciton-droplet cloud. We have neglected in (1) the exciton dragging by the phonon wind. In this approximation, the wind influences the spatial distribution of the excitons only via S_Σ.

Assume that the exciton "vapor" is saturated in some region $a < x < b$, i.e., $n(x) > n_{0T}$, where n_{0T} is the thermody-

namic-equilibrium density of the saturated vapor and is defined by

$$n_{0T}=v_d(m_d kT/2\pi\hbar^2)^{3/2}\exp\,(-\varphi_0/kT),\tag{2}$$

where v_d is the degeneracy multiplicity of the exciton ground state, m_d is the effective mass of the exciton density of states, and φ_0 is the work function of the exciton from the electron-hole liquid (EHL). The density of the nuclei having a critical radius

$$R_{cr}=\frac{2\beta\varphi_0}{kT\ln(n(x)/n_{0T})}n_0^{-1/3},\tag{3}$$

and produced per unit time depends locally on the supersaturation $[n(x)/n_{0T}]$ and is determined by the known Becker-Döring equation

$$I_{B-D}=A\left(\frac{\beta\varphi_0}{kT}\right)^{1/2}V_T n_0^{-2/3}N_{im}n(x)\exp\left\{-\frac{\lambda}{\ln^2(n(x)/n_{0T})}\right\}.\tag{4}$$

In (3) and (4), $\beta=\sigma/\varphi_0 n_0^{2/3}$, σ is the surface-tension coefficient, n_0 is the EHL density, A is a dimensionless parameter, $V_T=(kT/2\pi M)^{1/2}$ is the exciton thermal velocity, M is their effective mass, N_{im} is the condensation-center density, and $\lambda=(2\pi/3)(2\beta\varphi_0/kT)^2$. Strictly speaking, since the EHL lifetime is short, Eq. (4) is valid only at not too low EHL temperatures $(T\gtrsim 2$ K$)$ and at relatively high gas supersaturation.[33,23]

Once produced, the nuclei begin to grow and are simultaneously accelerated in the force field of the phonon wind. Since both the force exerted on the droplets by the phonon wind and the friction with the lattice are proportional to the number of particles, the nuclei are accelerated to a certain velocity V that is independent of their size and is determined by the phonon-wind intensity and by the lattice temperature. The velocity V assumes its steady-state value within a rather short time, on the order of the EHD momentum-relaxation time $\tau_r\sim 10^{-9}$ s (Ref. 34). We shall therefore assume that after they are produced the nuclei instantaneously acquire a specified velocity, the value of which we subject to a single limitation: it must be small compared with the thermal velocity of the excitons, $V\ll V_T$. The last limitation simplifies greatly the subsequent calculations and means that the excitons are condensed on the surfaces of the moving droplets as if the latter were immobile. The rate of exciton condensation into a liquid phase is then given by

$$S_\Sigma(x)=\Sigma(x)V_T[n(x)-n_{0T}]+\tfrac{4}{3}\pi R_{cr}^3(x)n_0 I_{B-D}(x),\tag{5}$$

where $\Sigma(x)$ is the total area of the droplet surface per unit volume at the point x. The second term in the right-hand side of (5) describes the decrease of the exciton density owing to formation of critical nuclei. We note that this term was disregarded in Ref. 28. In our case, however, as will be shown below, the droplet motion causes redistribution of the density, and the contribution of this term at large supersaturation can be significant.

The droplet sizes at a point x will generally speaking depend on where the given droplet was produced. Let $R(x,x')$ be the radius of a droplet produced at a point x' and located at the considered instant of time at the point x. Tak-

ing the foregoing into account, the equation for $R(x,x')$ is of the form[28]

$$V\frac{\partial R(x,x')}{\partial x}=\frac{n(x)-n_{0T}}{n_0}V_T-\frac{R(x,x')}{3\tau_0},\tag{6}$$

where τ_0 is the lifetime of the carriers in the EHL. (Recall that we are considering the steady state: $\partial R/\partial t=0$.) The first term in the right-hand side of (6) describes condensation and evaporation of the carriers from the droplet surface, and the second their recombination inside the droplet. Note that we have neglected in (5) and (6) the contribution of the surface energy the work function of the excitons from the HED.[26,28] Equation (6) must be supplemented by the obvious boundary condition

$$R(x,\,x)=R_{cr}(x).\tag{7}$$

Integrating (6) with (7) taken into account we obtain

$$R(x,x')=\exp\left\{-\frac{x-x'}{3\tau_0 V}\right\}$$
$$\times\left\{\frac{V_T}{V}\int_{x'}^{x}\exp\left\{\frac{\xi-x'}{3\tau_0 V}\right\}[n(\xi)-n_{0T}]d\xi+R_{cr}(x')\right\}.\tag{8}$$

The total surface area of the droplets per unit volume, at the point x, is

$$\Sigma(x)=\begin{cases}0, & x\leqslant a\\[2mm]4\pi\int_a^x R^2(x,x')(\partial N_d/\partial x')dx', & x>a\end{cases}\tag{9}$$

From the continuity equation it follows for our case that

$$\frac{\partial N_d(x')}{\partial x'}=\frac{1}{V}I_{B-D}(x');\tag{10}$$

here $N_d(x)$ is the droplet density at the point x.

This completes the derivation of the closed equation for the density of the exciton "vapor." This equation takes the form

$$D\frac{d^2n(x)}{dx^2}+g(x)-\frac{n(x)}{\tau}-4\pi\frac{V_T}{V}[n(x)-n_{0T}]\int_a^x I_{B-D}(x')$$
$$\times R^2(x,x')dx'-\frac{4\pi}{3}n_0 R_{cr}^3(x)I_{B-D}(x)=0.\tag{11}$$

Here $R(x,x')$ is an integral of $n(x)$ similar to (8), and the dependence of I_{B-D} on $n(x)$ is given by Eq. (4).

Equations (4), (8), and (11) form a complete system of equations that describe exciton condensation for uniform drift motion of EHD at a given velocity. In principle, if the function $g(x)$ is known, we can obtain from these equations all the basic macroscopic parameters that characterize the exciton-droplet cloud, viz., the distribution of the exciton density $n(x)$ over the volume of the sample, the average density of the carriers bound into droplets (the volume of the liquid phase)

$$\bar{n}(x)=\frac{4}{3}\pi n_0\int_a^x R^3(x,x')\frac{\partial N_d(x')}{\partial x'}dx',\tag{12}$$

the droplet density
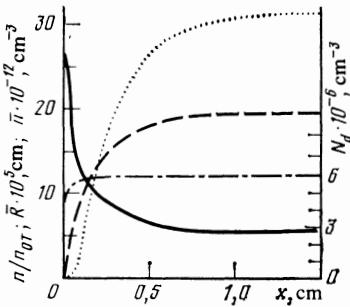
FIG. 1. Calculated spatial distributions of the ratio n/n_{0T} of the exciton density and saturated-vapor densities (solid curve), of the EHD density N_d (dash-dot) and average radius R (dashed), and of the average liquid-phase-particle density n (dotted) for a semi-infinite generation region. The calculation was carried out for $V = 10^4$ cm/s, $g = 10^{18}$ cm^{-3} s^{-1}, $\tau_0 = 4 \cdot 10^{-5}$ s, $T = 2$ K, $n_{0T} = 1.92 \cdot 10^{11}$ cm^{-3} and $V_T = 3.3 \cdot 10^5$ cm/s (the numerical values of the remaining temperature-independent quantities are given in the footnote of Table I).

$$N_d(x) = \int_a^x \frac{\partial N_d(x')}{\partial x'} dx', \qquad (13)$$

the average droplet radius

$$\bar{R}(x) = [3\bar{n}(x)/4\pi n_0 N_d(x)]^{1/3}, \qquad (14)$$

and also the EHD-radius distribution for each point of the sample.

Before we proceed to the analysis of the solution of the system (4), (8), and (11) at specified excitation conditions, we make a few remarks of general character. It was shown in Ref. 28 that under stationary excitation the steady-state values of the exciton density, as well as the densities and radii of the EHD, depend on the rate of application of the excitation, i.e., the exciton-droplet system preserves memory of the conditions under which the EHD were produced and grew. This is precisely why hysteresis phenomena can be observed near the EHD-formation threshold.[35,36,33] In our case, however, owing to the drift of the EHD, the memory of the initial conditions is erased and a new stationary state sets in, in which the functions $n(x)$, $\bar{n}(x)$, $N_d(x)$, and $\bar{R}(x)$ depend on the EHD drift velocity. It is therefore impossible to go in Eq. (11) to the limit of the static regime ($V = 0$). It appears that the singularities observed in Refs. 42 and 43 in the excitation and absorption of EHD radiation upon application of the excitation are due to restructuring of the exciton-droplet system and its transition to a new stationary state.

At constant drift velocity the path length of the droplets is directly proportional to the time, and the produced spatial picture is in fact a linear time scan of the condensation process. An interesting possibility offers itself of investigating experimentally the exciton-condensation kinetics (as well as EHD recombination kinetics),[22] viz., measurements of the coordinate dependences of $n(x)$, $\bar{n}(x)$, $N_d(x)$ and $\bar{R}(x)$ under EHD drift conditions should yield essentially the same data as temporal measurements of the quasistationary excitation on the leading (trailing) edge of the pulse. Further, by varying the drift velocity we can control the nucleation and growth of the EHD.

It must also be emphasized that the drift of the EHD

leads not only to a coordinate dependence of the droplet radius, but also to the onset of a droplet distribution in size at each point x of the sample. This is seen directly from Eq. (6) and its cause is that the EHD that are present at a given point x were produced at all points with coordinates $x' < x$. It appears that the EHD size distribution observed under intense stationary[44] and pulsed[45] pumping is formed mainly as a result of droplet dragging by the phonon wind.[22]

We investigate now the qualitative features of the simultaneous solution of Eqs. (4), (8), and (11) at different values of the parameters g, V, and others. We consider for simplicity only situations in which the diffusion term in Eq. (11) can be neglected. The nondiffusion approximation can be used if the solution $n(x)$ is a sufficiently smooth function over distances of the order of the exciton-diffusion length $L_D = (D\tau)^{1/2}$. Satisfaction of this condition will be verified in each case.

1. Homogeneous excitation. In the entire sample, which fills the half-space $g \geqslant 0$, we have $g(x) = g = $ const ($g > n_{0T}/\tau$, otherwise no EHL is produced and solution (11) is trivial: $n = g\tau$).

We note first the following important circumstance: the left-hand side of Eq. (11) depends in this case on x either via the combination x/V or via the function $n(x)$, and can be symbolically written in the form

$$F[x/V, n_V(x')] = 0, \qquad (15)$$

where the superscript V of $n(x)$ shows that the solution $n_V(x)$ corresponds to a drift velocity V. Writing down (15) for the velocity αV, where α is any real number, we find that $n_{\alpha V}(\alpha x) = n_V(x)$, i.e., in the no-diffusion approximation the distributions $n_{V_1}(x_1)$ and $n_{V_2}(x_2)$ that are established in the system at two different droplet drift velocities V_1 and V_2 agree to within the scale transformation $x_1 = x_2 V_1/V_2$. This is perfectly natural, since the problem has no parameter with dimension of length at $g = $ const. It follows hence, in particular, that the no-diffusion approximation holds well, at any rate at high drift velocities V.

Let us consider this question in somewhat greater detail. The largest change of the function $n(x)$ occurs near the origin (Fig. 1). We shall therefore investigate its behavior in this region. At $x = 0$ the integral term in (11) vanishes and the value of the boundary plane $n(0)$ is obtained from an algebraic equation that is independent of $V(y_0 = n(0)/n_{0T}$, $y_m = g\tau/n_{0T})$:

$$y_m - y_0 = \frac{32}{3}\pi\left(\frac{\beta\varphi_0}{kT}\right)^{1/2}\frac{V_T\tau N_{tm}}{n_0^{1/3}}\frac{y_0}{\ln^3 y_0}\exp\left\{-\frac{\lambda}{\ln^2 y_0}\right\}. \qquad (16)$$

At small $x \ll x_0$ the solution (11) takes the form

$$n(x) = n_{0T} y_0(1 - x/x_0), \qquad (17)$$

where

$$x_0 = \left|\frac{n(0)}{n'(0)}\right|$$
$$= \frac{2}{3}\frac{V}{V_T}\left(\frac{\beta\varphi_0}{kT}\right)\frac{n_0^{2/3}}{n_{0T}}\frac{y_0 + (y_m - y_0)(1 + 2\lambda/\ln^3 y_0 - 3/\ln y_0)}{\ln y_0(y_0 - 1)(y_m - y_0)}. \qquad (18)$$

For the no-diffusion approximation to be valid it is necessary
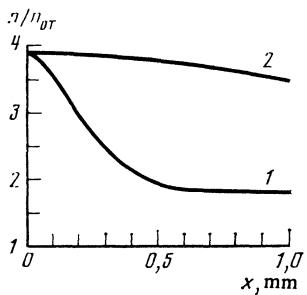
FIG. 2. Calculated dependences of the relative exciton-gas density on the distance to the generation-region boundary (1—$V = 8 \cdot 10^2$ cm/s, 2— $V = 8 \cdot 10^3$ cm/s). The calculation was carried out at $g = 1.5 \cdot 10^{19}$ cm$^{-3} \cdot$s^{-1} and $T = 3$ K (the numerical values of the remaining quantities are given in the footnote of Table I).

to satisfy the condition $x_0 \gg L_D$. Since $x_0 \propto V$, this can occur, as already indicated, at sufficiently large V (Fig. 2). On the other hand, this approximation can be used at relatively small supersaturation of the exciton "vapor": $1 < y_m \lesssim 10$. In this case the right hand side of (16) is very small, in view of the smallness of the exponential factor, therefore $y_0 \cong y_m$ and

$$x_0 \approx \frac{1}{16\pi} \left(\frac{kT}{\beta \varphi_0} \right)^{5/2} \frac{n_0^{4/3}}{n_{0T}\tau N_{im}} \frac{V}{V_T^2} \frac{\ln^2 y_m}{y_m - 1} \exp\{\lambda / \ln^2 y_m\}. \quad (19)$$

It is seen from Eq. (19) that x_0 increases exponentially rapidly with decreasing supersaturation; in particular, at $y_m = 1 + \delta$, where $\delta \ll 1$, we have $x_0 \propto \delta \exp(\lambda / \delta^2) \gg 1$. To illustrate the foregoing, Table I lists the values of y_0 and x_0 numerically calculated from Eqs. (16) and (18).

We present now approximate relations for the connection between the steady-state values of R, n, and N_d at large x. In this case

$$n(x) = n_\infty, \quad dn/dx = 0, \quad \partial R(x, x')/\partial x = \partial R(x, x')/\partial x' = 0$$

and it follows from (6) that the equation for the droplet radius takes the usual form[40]

$$R_\infty = \frac{3\tau_0}{n_0} (n_\infty - n_{0T}) V_T. \quad (20)$$

The steady-state exciton density n_∞ is connected with the steady-state droplet density

$$N_{d\infty} = \frac{1}{V} \int_0^\infty I_{B-D}(x)\,dx$$

by the cubic equation

$$z_\infty^3 + \frac{1}{\Phi} z_\infty - \frac{1}{\Phi} z_m = 0, \quad (21)$$

with

$$z_\infty = (n_\infty - n_{0T})/n_{0T}, \quad z_m = y_m - 1, \quad \Phi = 36\pi\tau_0^2 \tau V_T^3 \cdot (n_{0T}/n_0)^2 N_{d\infty},$$

whose solution is

$$z = z_m \left\{ \left[\frac{1}{2\Phi z_m} \left(1 + \left(1 + \frac{4}{27} \frac{1}{\Phi z_m^2} \right)^{1/2} \right) \right]^{1/3} \right.$$
$$\left. + \left[\frac{1}{2\Phi z_m} \left(1 - \left(1 + \frac{4}{27} \frac{1}{\Phi z_m^2} \right)^{1/2} \right) \right]^{1/3} \right\}. \quad (22)$$

If $\Phi z_m^2 \gg 1$, then

$$z_\infty \approx z_m / (\Phi z_m^2)^{1/3}. \quad (23)$$

$z_\infty \approx 0$ in the opposite limiting case $\Phi z_m^2 \ll 1$.

We present, finally, the results of the numerical solution of the system (4), (8), and (11). Figure 1 shows the spatial distributions of the exciton-gas density, of the average density of the carriers bound into droplets [Eq. (12)], and the droplet density [Eq. (13)], and average radius [Eq. (14)]. These relations can be qualitatively explained as follows. Since the droplets move in the opposite direction of the x axis, the EHD nuclei produced in the volume of the crystal are located near the boundaries of the generation region ($x = 0$), and leave this volume before they can absorb a noticeable number of excitons. The droplet motion into the interior of the excitation region is accompanied by an increase of their radius and accordingly by an increase of the total EHD surface defined by Eq. (9). This leads to an increase of the exciton flux to the surfaces of the droplets [Eq. (5)] and to a decrease of the exciton density with increasing distance from the boundary of the generation region. Owing to the strong dependence of the rate of formation of critical nuclei on the supersaturation of the exciton "vapor" [Eq. (4)], new droplets are nucleated in a relatively narrow region near $x = 0$, where the exciton density is a maximum, and the droplet density N_d assumes the steady-state value $N_{d\infty}$ at relatively short distances from the $x = 0$ plane. The EHD produced in this region still continue to grow for some time as they move inside the crystal, until the exciton-gas density and the EHD radii reach their steady-state values n_∞ and R_∞ determined by Eqs. (22) and (20), respectively.

TABLE I. Numerical values of y_0 and x_0 for various excitation levels at $T = 3$ K and $V = 8 \cdot 10^3$ cm/s.

g	$y_m = g\tau_0/n_0 T$	$y_0 = n(0)/n_0 T$	$x_0 = [n(0)/n'(0)]$, cm	L_D/x_0
10^{19}	2.44	2.44	210	$4 \cdot 10^{-4}$
$1.5 \cdot 10^{19}$	3.87	3.87	110	$8 \cdot 10^{-4}$
$2.5 \cdot 10^{19}$	6.14	6.14	0.5	0.18
$4 \cdot 10^{19}$	9.73	9.67	$3 \cdot 10^{-3}$	28 *
$6.3 \cdot 10^{19}$	15.4	14.6	$2 \cdot 10^{-4}$	430 *

Note. The numerical values used for the quantities that enter in Eqs. (16) and (18) and in the relation $L_D = (D\tau)^{1/2}$ are: $n_{0T} = 2.04 \cdot 10^{13}$ cm^{-3}, $V_T = 4.05 \cdot 10^5$ cm/s, $\sigma = 2 \cdot 10^{-4}$ erg/cm^2, $\varphi_0 = 2.1$ meV, $n_0 = 2 \cdot 10^{17}$ cm^{-3}, $M = 4 \cdot 10^{-28}$ g, $N_{im} = 10^{12}$ cm^{-3}, $\tau = 5 \cdot 10^{-6}$ s and $D = 1500$ cm^2/s.

*The no-diffusion approximation is not valid: $L_D/x_0 > 1$.

FIG. 3. Stationary spatial distributions: a) of the relative generation rate $(g\tau/n_{0T})$ and of the exciton-gas density (n/n_{0T}); b) of the droplet density (N_d); c) of the average EHD radius $(\bar{R})$, and d) of the average density $\bar{n}\cdot10^{-13}$ cm^{-3} of the carriers bound into drops. 1) $V = 10^2$ cm/s, 2) $V = 10^3$ cm/s, 3) $V = 10^4$ cm/s.

We note that although in the transition region the EHD vary in size, the droplet radii become equalized, as $x \to \infty$, since the exciton density and the EHD radius are uniquely related by Eq. (20).

It is clear from the foregoing that an increase of the EHD drift velocity should expand the transition region (i.e., the region in which the EHD are nucleated and grow). This is illustrated by Fig. 2.

2. Generation region of limited size (in the z direction). If homogeneous excitation is effected in a region $0 < x < b$ with abrupt boundaries, the spatial distributions of n, N_d, $\bar{R}$, and $\bar{n}$ inside the generation region will be in the no-diffusion approximation the same as in a semi-infinite region at $x < b$ (Figs. 1 and 2). Outside the generation region $(x > b)$ the density of the droplets moving along the x axis will remain constant and equal to $N_d(x = b)$ practically until the droplets that decrease in size by evaporation and by recombination of their constituent particles vanish. At the same time, the exciton density will differ from zero in the region $x > b$ on account of evaporation of the EHD. We shall not go here into details of this case, and present for the system Eqs. (4), (8), (11) a numerical solution that corresponds to generation in a bounded region with smooth boundaries (Fig. 3). The spatial distribution of the generation rate was calculated from the equation

$$g(x) = 2g_{max}/(e^{x/a} + e^{-x/a}) \quad (24)$$

with $g_{max} = 1.9\cdot10^{-19}$ cm$^{-3}\cdot$s^{-1} and $a = 0.1$ cm (i.e., $a \approx L_D$). Calculations for $T = 2.5$ ($V_T = 3.7\cdot10^5$ cm/s, $n_{0T} = 3.07\cdot10^{12}$ cm^{-3}, the numerical values of the remaining temperature-independent quantities are given in the footnote of Table I and in the caption of Fig. 1). From a comparison of the data shown in Figs. 3a and 3b it can be seen that at $T = 2.5$ K the rate of formation of EHD nuclei becomes appreciable when the supersaturation of the exciton "vapor" is $n/n_{0T} \approx 5$ (horizontal section of curve 1 of Fig. 3a). At low drift velocities, the EHD and their surrounding exciton gas have time to enter into equilibrium, and the EHD radius is given by Eq. (20) with the substitution $n_\infty \to n(x)$. In the left-hand part $(x < 0)$ of the excitation region, notwithstanding the increase of the generation rate with increasing x, the exciton density, and with it also the EHD radius (Fig. 3c), stabilize on a constant level (Fig. 3a, curve 1), so that the growth of this density is restricted by the strong dependence of the rate of critical-nucleus formation[5] on n/n_{0T}. In the region $x > 0$ the rate of generation decreases with increasing x, not enough excitons are produced here to maintain the dimensions of the entering EHD at the level corresponding to the center of the excitation region, and the EHD radii (Fig. 3c), the exciton density (Fig. 3a), and the liquid-phase volume (Fig. 3d) decrease with increasing x at practically constant EHD density (Fig. 3b).

Increasing the drift velocity (curves 2 and 3 of Fig. 3) changes the situation substantially. Just as in the case of homogeneous generation in a semi-infinite volume, the exciton density near the left-side boundary of the excitation region increases, as does the size of the region of increased exciton-gas density, with increasing EHD velocity (Fig. 3a). The droplets are nucleated only in this region (Fig. 3b), and at sufficiently high drift velocities their growth continues practically during the entire time of motion through the excitation region (curve 3 of Fig. 3c). It can then be seen from curves of Figs. 3a and 3b that no equilibrium is established between the EHD and the exciton gas: as the droplets move their radius increases despite the decrease in the exciton density.

EXPERIMENT

The measurements were performed with the apparatus described in detail in Ref. 47. The experimental geometry is shown in the inset of Fig. 4. The bulk-excitation source was a helium-neon laser of ~ 10 mW power, operating at a wavelength 1.52 μm. The exciting radiation was modulated at 1 kHz and focused on the front surface of the sample into a spot of ~ 200 μm diameter. The pump pulse rise and fall times were ≈ 100 μs.

We measured the absorption and scattering of 3.39-μm He–Ne laser radiation. This radiation was also focused on the front surface of the sample into a spot of ~ 300 μm diameter. Exact superposition of the two spots occurred when the absorption signal was a maximum.

The radiation scattered by the EHD was amplified with a helium–neon laser amplifier and recorded with a PbS receiver cooled to ~ 100 K. The angular distribution of the scattered-light intensity was automatically plotted on an x–y
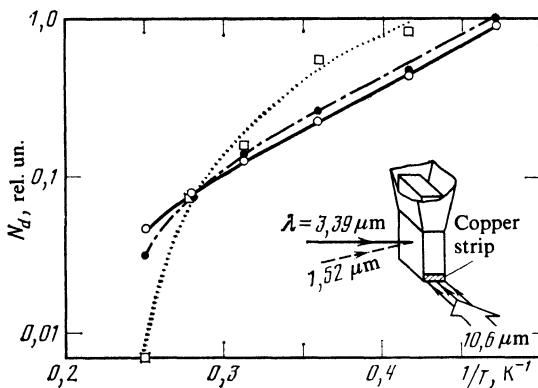
FIG. 4. EHD density vs reciprocal temperature, $P_{max} = 100$ mW. P/P_{max} = 0 (O), 0.3 (●), and 1.0 (□). Inset—experimental geometry.

recorder chart.

Simultaneously with the scattering measurements we recorded the germanium recombination-radiation spectrum. To observe luminescence we used a standard setup with a large-aperture MDR-2 monochromator. The radiation was recorded with a cooled PbS photoresistor. Just as in Ref. 28, we analyzed the recombination radiation emerging through a lateral surface of the sample—the monochromator slit passed a beam 0.3 mm wide near the sample's front surface.

The thermal generator of nonequilibrium phonons was an uncompact copper strip deposited on a lateral surface of the sample and continuously illuminated by a CO_2 laser ($\lambda = 10.6\,\mu m$) with a maximum power $P_{max} \approx 100$ mW.

The measurements were performed on mechanically polished germanium samples with residual impurity density not higher than 10^{12} cm^{-3}. To exclude the light scattered by the boiling-helium bubbles, samples measuring $15 \times 5 \times 3$ mm were fused into the bottom of the cryostat's helium vessel in such a way that the working half of the sample was in a vacuum.

EXPERIMENTAL RESULTS AND DISCUSSION

Figure 5 shows plots of the exciton (a) and EHD (b) recombination-radiation intensity, and of the EHD density (c), measured by the light-scattering method, versus the power P of the radiation that heated the copper strip. In
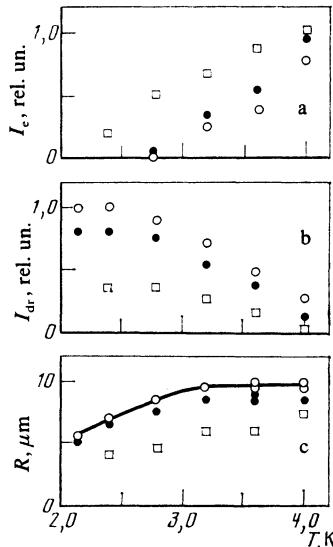
FIG. 6. Temperature dependences of the exciton (a) and EHD recombination radiation (b) intensities and of the EHD radius (c). $P_{max} = 100$ mW, $P/P_{max} = 0$(O), 0.3 (●); 1.0 (□).

actual fact these are plots of the aforementioned quantities vs the EHD drift velocity, the latter being proportional the density of the phonon-energy flux directed from the heater to the excitation region and proportional to P. At $P = P_{max}$ = 100 mW the drift velocity was ~ 10^3 cm/s at $T = 2.4$ K.[6] This estimate of the velocity was obtaining by measuring the EHD drift path.[1] It can be seen from Figs. 5a, 5b, 6a, and 6b that when the EHD drift velocity is increased the number of excitons in the excitation region increases, and the volume of the liquid phase decreases. The exciton-density change is larger at low temperature, whereas the average density of the particles bound into droplets undergo the greatest changes in the high-temperature region. It is interesting that, depending on the sample temperature, the EHD density can either increase or decrease with increasing phonon-wind intensity (Figs. 5c and 4). At the same time, the droplet radius always decreases with increasing EHD drift velocity (Fig. 6c).

We proceed now to analyze the results on the basis of the above condensation theory that takes into account drop-
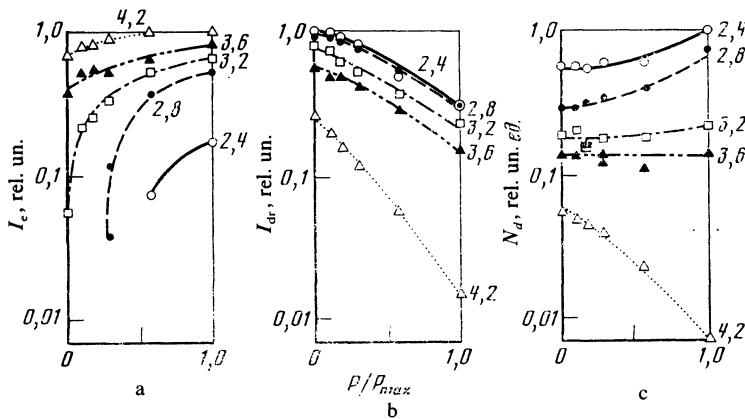
FIG. 5. Luminescence intensities I_c of the excitons (a) and I_{dr} of the EHD (b), and EHD density N_d (c), vs the radiation power incident on a metallic strip. $P_{max} \approx 100$ mW. The numbers at the curves are the temperatures in K.

let motion through an exciton cloud. We note first that these results cannot be attributed to sample heating by the laser used to generate the phonon wind. Indeed, although the exciton-gas density and the liquid-phase volume behave when P is increased (Figs. 5a, b) in the same manner as when the temperature is raised (Figs. 6a, b), the plots of the EHD density and radius versus p show that the relations observed are not connected with the heating. When P is increased the EHD radius decreases (Fig. 6c), and the EHD density increases at low temperature (Fig. 5c), whereas raising the sample temperature increases the radius (Fig. 6c) and decreases the density (Fig. 4) of the EHD. The observed change of the relations between the mean densities of the liquid and gas phases can thus be attributed to the EHD motion.

As shown above, the EHD motion produces regions of increased exciton density in the excited sample volume. These regions expand with increasing drift velocity (Figs. 1, 2, and 3a). The data shown in Fig. 5a are a direct confirmation of this circumstance. Since the increase of the exciton density is connected with the fact that the EHD motion does not leave the excitons enough time to condense on the droplet surface, the increase of the exciton density with increase of P should be more intense at low temperatures than at high ones, inasmuch as almost all nonequilibrium carriers are in the gas phase at high temperature.

The observed decrease of the EHD size with increasing P (Fig. 6c) agrees qualitatively with the calculation result (Fig. 6c) and is due to two circumstances. First, at sufficiently high velocities the EHD leave the exciton cloud before they manage to grow to the size they would reach in the absence of motion (this is in fact the cause of the decrease of the EHD radius at high temperatures). Second, at low temperatures the decrease of the EHD radius is due to the increased droplet density (Fig. 5c), in analogy with the case when the exciting-pulse rise time is shortened.[28] It is interesting to note that at high velocities the EHD radius increases practically linearly with temperature, whereas in the absence of EHD drift (and also at low EHD velocities, Fig. 6c), the droplet radius is independent of temperature in the high-temperature region.[28]

From the results shown in Figs. 5b, 5c, and 6c it can be seen that the decrease of the liquid-phase volume with increase of droplet drift velocity is due at low temperatures to the decreased size of the EHD, and at high velocities with decreases of both the radius and the density of the EHD. It was noted in the interpretation of the calculation results that at sufficiently high drift velocities there is not enough time for equilibrium to be established between the liquid and the gas in the excitation region. The experimental data (Figs. 6a and 6b) also point to this circumstance: when the EHD velocity is increased the temperature dependences of the exciton and EHD luminescence intensities (meaning also the mean particle densities in the gas and liquid) become weaker.

Let us examine, finally, the behavior of the EHD density (Figs. 5c and 4). A stationary EHD density is established in the excitation region when a balance is reached between the number of EHD drops produced in this region and the number of drops that drift out of it. Assuming approximately that the excitons and the EHD are uniformly distributed in the excitation region, we obtain with the aid of Eq. (10) $N_d = I_{B-D} b / V$, where b is the width of the generation region. At low temperatures the strong increase of the exciton density with increasing velocity V (Fig. 5a) leads according to (4) to a sharp increase of the rate I_{B-D} of EHD nucleation, and with it to an increase of the droplet density (the calculated N_d are shown in Fig. 3b). At high temperatures the exciton-gas density depends little on the phonon-wind intensity (Fig. 5a), and therefore N_d decreases with increasing drift velocity (Figs. 5c and 4). It was noted above that the drift-induced spatial distributions of the excitons and of the EHD correlate with the time dependences of n, N_d, R, and $\bar{n}$ during the establishment of the steady state after the excitation is turned on. For example, an increase of the drift velocity in experiments on the spatial dependences leads to the same qualitative changes of the macroscopic liquid-phase parameters (EHD sizes and density) as a shortening of the rise time of the excitation pulse in experimental investigations of the condensation kinetics following application of the excitation. This can be seen directly by comparing our present results with the data of Ref. 28: faster turning-on of the excitation increases substantially the droplet density at low temperatures, whereas in the high-temperature region (when the supersaturation is decreased) the dependence of the density on the front rise time becomes weaker.

We present no quantitative reconciliation of the experimental results with the theoretical equations since, first, we do not know the spatial distribution of the generation rate and, second, exciton diffusion and droplet dragging by the phonon wind can alter substantially the spatial distributions of the experimental quantities. The theory expounded above, however, provides a correct qualitative description of all the main features of the results, i.e., the manner in which the macroscopic liquid-phase parameters, averaged over the excitation region and the exciton-gas density depend on the EHD drift velocity at various crystal temperatures.

CONCLUSION

We have described above the results of theoretical and experimental investigations of exciton-condensation kinetics under conditions when the droplets drift through an exciton cloud. The theory considered is suitable for the description of the kinetics in a exciton-gas + EHD system in various experiments, when the droplets acquire a one-dimensional directed motion by one method or another (EHD dragging by phonon wind,[1] non-uniform deformation of the sample,[37,38] dragging by ultrasound,[39] and others). This theory can be used also for a qualitative analysis of EHD nucleation and growth at sufficiently high stationary-excitation levels, when the spatial distribution of the EHD is determined by the dragging of the droplets by phonon wind.[22] This situation is realized under conditions of the majority of experiments with EHD (except for experiments aimed at observing optical hysteresis[33]). The result lead to a rather interesting deduction: droplet motion can be used as a time

1280   Sov. Phys. JETP 62 (6), December 1985

Zamkovets et al.   1280

scan of the condensation and recombination processes, and information on the kinetics of these processes can be obtained by measuring, with spatial resolution, the macroscopic parameters of the liquid phase. The results of an experimental investigation of the condensation kinetics when droplets are dragged by nonequilibrium phonons emitted by a heat generator confirm qualitatively the main deductions of the theory.

We are deeply grateful to V. S. Bagaev and L. V. Keldysh for interest and numerous helpful discussions.

---

[1] A detailed discussion of the influence of phonon wind on the properties of a system of EHD and an almost complete bibliography on this subject can be found in the reviews by Bagaev *et al.*[22] and by Tikhodeev.[23]

[2] Excitons are much less strongly dragged by phonons than EHD (at least in germanium[11] and their drift can be disregarded. In CdS, however the dynamics of the exciton cloud is determined by the dragging of excitons by nonequilibrium phonons.[24]

[3] Condensation kinetics is most exhaustively described in the reviews by Rice *et al.*[34] and by Tikhodeev.[23]

[4] The conditions imposed on the smoothness of $n(x)$ will be made more precise below.

[5] A similar situation obtains in experiments on optical hysteresis. When the generation rate is increased, the liquid-phase volume increases mainly because the EHD density rather than its size increases.[33] These experiments are carried at such low pump levels that the phonon-wind force is insufficient to separate the droplets from the impurities.[46]

[6] Given the phonon-wind intensity, the drift velocity decreases when the temperature is raised, owing to the decreased EHD mobility.[48,22,23]

---

[1] V. S. Bagaev, L. V. Keldysh, N. N. Sibel'din, and V. A. Tsvetkov, Zh. Eksp. Teor. Fiz. **70**, 702 (1976) [Sov. Phys. JETP **43**, 362 (1976)].

[2] L. V. Keldysh, Pis'ma Zh. Eksp. Teor. Fiz. **23**, 100 (1976) [JETP Lett. **23**, 86 (1976)].

[3] J. C. Hensel and R. C. Dynes, Phys. Rev. Lett. **39**, 969 (1977). Proc. 14th Int. Conf. Physics of Semiconductors, 1978, B. L. Wilson, ed., Inst. Phys. Conf. Ser. No. 43, Bristol and London (1979), p. 372.

[4] V. M. Asnin, A. A. Rogachev, N. I. Sablina, and V. I. Stepanov, Fiz. Tverd. Tela (Leningrad) **19**, 3150 (1977); **23**, 177 (1981) [Sov. Phys. Solid State **19**, 1844 (1977); **23**, 99 (1981)].

[5] T. A. Astemirov, V. S. Bagaev, L. I. Paduchikh, and A. G. Poyarkov, Pis'ma Zh. Eksp. Teor. Fiz. **24**, 225 (1976) [JETP Lett. **24**, 200 (1976)].

[6] T. C. Damen and J. M. Worlock, Proc. Third Int. Conf. on Light Scattering in Solids, Campinas, Brazil, 1975 (Flammarion, Paris, 1976), p. 183.

[7] J. Doehler, J. C. Mattos, and J. M. Worlock, Phys. Rev. Lett. **38**, 726 (1977).

[8] A. D. Durandin, N. N. Sibel'din, V. B. Stopachinskii, and V. A. Tsvetkov, Pis'ma Zh. Eksp. Teor. Fiz. **26**, 395 (1977) [JETP Lett. **26**, 272 (1977)].

[9] N. V. Zamkovets, N. N. Sibel'din, V. B. Stopachinskii, and V. A. Tsvetkov, Zh. Eksp. Teor. Fiz. **74**, 1147 (1978) [Sov. Phys. JETP **47**, 603 (1978)].

[10] J. Doehler and J. M. Worlock, Phys. Rev. Lett. **41**, 980 (1978).

[11] M. Greenstein and J. P. Wolfe, *ibid.* p. 715.

[12] M. Greenstein and J. P. Wolfe, Sol. St. Comm. **33**, 309 (1980).

[13] R. S. Markiewicz, M. Greenstein, and J. P. Wolfe, *ibid*, **35**, 339 (1980).

[14] M. Greenstein and J. P. Wolfe, Phys. Rev. B **24**, 3318 (1981).

[15] J. P. Wolfe, R. S. Markiewich, S. M. Kelso, J. E. Furneaux, and C. D. Jeffries, *ibid.* B **18**, 1479 (1978).

[16] R. S. Markiewich, Sol. St. Comm. **33**, 701 (1980).

[17] R. S. Markiewich, Phys. Rev. B **21**, 4674 (1980).

[18] M. A. Tamor, M. Greenstein, and J. P. Wolfe, *ibid.* B **27**, 7353 (1983).

[19] I. V. Kavetskaya, N. N. Sibel'din, V. B. Stopachinskii, and V. A. Tsvetkov, Fiz. Tverd. Tela (Leningrad) **20**, 3608 (1978) [Sov. Phys. Solid State **20**, 2085 (1978)].

[20] N. N. Sibel'din, V. B. Stopachinskii, S. G. Tikhodeev, and V. A. Tsvetkov, Pis'ma Zh. Eksp. Teor. Fiz. **38**, 177 (1983) [JETP Lett. **38**, 207 (1983)].

[21] S. J. Kirch and J. P. Wolfe, Phys. Rev. B **29**, 3382 (1984).

[22] V. S. Bagaev, T. I. Galkina, and N. N. Sibeldin, in: Modern Problems in Condensed Matter Sciences (gen. eds. V. M. Agranovich and A. A. Maradudin), North-Holland, 1983, Vol. 6 (Electron-Hole Droplets in Semiconductors, C. D. Jeffries and L. V. Keldysh, eds.), Chap. 4, p. 267.

[23] S. G. Tikhodeev, Usp. Fiz. Nauk **145**, 3 (1985) [Sov. Phys. Usp. **28**, 1 (1985)].

[24] N. N. Zinov'ev, L. P. Ivanov, V. I. Kozub, and I. D. Yaroshetskii, Zh. Eksp. Teor. Fiz. **84**, 1761 (1983) [Sov. Phys. JETP **57**, 1027 (1983)].

[25] V. S. Bagaev, N. V. Zamkovets, N. N. Sibel'din, S. G. Tikhodeev, and V. A. Tsvetkov, Abstracts, All-Union Conf. "Excitons and Semiconductors '82," Leningrad, 1982, p. 77.

[26] R. N. Silver, Phys. Rev. B **11**, 1569 (1975).

[27] R. N. Silver, *ibid.* B **12**, 5689 (1975).

[28] V. S. Bagaev and S. G. Tikhodeev, Kratk. Soobshch. Fiz. (FIAN), No. 8, 9 (1976).

[29] R. M. Westervelt, Phys. Stat. Solidi (b) **74**, 727 (1976); **76**, 31 (1976).

[31] J. L. Staehli, *ibid.* (b). **75**, 452 (1976).

[32] B. Etienne, C. Benoit a la Guillaume, and M. Voos, Phys. Rev. B **14**, 712 (1976).

[33] R. M. Westerveld, see Ref. 22, Chap. 3, p. 187.

[34] T. M. Rice, J. C. Hensel, T. G. Phillips, and G. A. Thomas, Solid State Physics, H. Ehrenreich, F. Seitz, and D. Turnbull, eds., Academic, NY, 1977, Vol. 32.

[35] T. K. Lo, B. J. Feldman, and C. D. Jeffries, Phys. Rev. Lett. **31**, 224 (1973).

[36] R. M. Westervelt, J. L. Staehli, and E. E. Haller, Phys. Stat. Sol. (b). **90**, 557 (1978).

[37] V. S. Bagaev, T. I. Galkina, O. V. Gogolin, and L. V. Keldysh, Pis'ma Zh. Eksp. Teor. Fiz. **10**, 399 (1969) [JETP Lett. **10**, 254 (1969)].

[38] A. S. Alekseev, V. S. Bagaev, and T. I. Galkina, Zh. Eksp. Teor. Fiz. **63**, 1020 (1972) [Sov. Phys. JETP **36**, 536 (1973)].

[39] A. S. Alekseev, T. I. Galkina, V. N. Maslennikov, and S. G. Tikhodeev, *ibid.* **79**, 216 (1980) [**52**, 109 (1980)].

[40] Ya. E. Pokrovskii and K. I. Svistunova, Fiz. Tekh. Poluprov. **4**, 491 (1970) [Sov. Phys. Semicond. **4**, 409 (1970)].

[41] Ya. I. Frenkel', Kinetic Theory of Liquids, Dover, 1964.

[42] K. L. Shaklee, in Ref. 6, p. 160.

[43] T. M. Bragina, Yu. S. Lelikov, and Yu. G. Shreter, Zh. Eksp. Teor. Fiz. **79**, 1838 (1980) [Sov. Phys. JETP **52**, 929 (1980)].

[44] V. A. Zayats, V. N. Murzin, I. N. Salganik, and K. S. Shifrin, *ibid.* 73, 1422 (1977) [**46**, 748 (1977)].

[45] V. V. Katyrin, N. N. Sibel'din, V. B. Stopachevskii, and V. A. Tvetkov, Fiz. Tverd. Tela (Leningrad) **20**, 1426 (1978) [Sov. Phys. Solid State **20**, 820 (1978)].

[46] R. M. Westervelt, J. C. Culbertson, and B. S. Black, Phys. Rev. Lett. **42**, 267 (1979).

[47] V. S. Bagaev, N. V. Zamkovets, N. A. Penin, N. N. Sibel'din, and V. A. Tsvetkov, Prib. Tekh. Eksp. No. 2, 258 (1974).

[48] L. V. Keldysh and S. G. Tikhodeev, Fiz. Tverd. Tela (Leningrad) **19**, 111 (1977) [Sov. Phys. Solid State **19**, 63 (1977)].

Translated by J. G. Adashko